Modular determinants of antimicrobial activity in platelet factor-4 family kinocidins

Michael R. Yeaman [a,b,c,*], Nannette Y. Yount [a,c], Alan J. Waring [b,c], Kimberly D. Gank [a,c], Deborah Kupferwasser [a,c], Robert Wiese [d], Arnold S. Bayer [a,b,c], William H. Welch [d]

[a] *Division of Infectious Diseases, LAC-Harbor UCLA Medical Center, Torrance, CA 90509, USA*
[b] *Department of Medicine, David Geffen School of Medicine at UCLA, Los Angeles, CA 90025, USA*
[c] *St. John's Cardiovascular Research Center, Torrance, CA 90502, USA*
[d] *Department of Biochemistry, University of Nevada, Reno, NV 89557, USA*

Abstract

Mammalian platelets contain an array of antimicrobial peptides, termed platelet microbicidal proteins (PMPs). Human and rabbit PMPs include known chemokines, such as platelet factor-4 (hPF-4); PMP-1 is the rabbit orthologue of hPF-4. Chemokines that also exert direct antimicrobial activity have been termed kinocidins. A consensus peptide domain library representing mammalian PF-4 family members was analyzed to define structural domains contributing to antimicrobial activity against a panel of human pathogens. Secondary conformations were assessed by circular dichroism spectrometry, and molecular modeling was employed to investigate structural correlates of antimicrobial efficacy. Antimicrobial activity against isogenic peptide-susceptible or -resistant *Staphylococcus aureus*, *Salmonella typhimurium*, and *Candida albicans* strain pairs mapped to the C-terminal hemimer (38–74) and modular domains thereof (49–63 and 60–74). Increasing electrostatic charge and steric bulk were general correlates of efficacy. Structural data corroborated spatial distribution of charge, steric bulk and putative secondary structure with organism-specific efficacy. Microbicidal efficacies of the cPMP antimicrobial hemimer and C-terminal peptide (60–74) were retained in a complex human-blood biomatrix assay. Collectively, these results suggest that modular determinants arising from structural components acting independently and cooperatively govern the antimicrobial functions of PF-4 family kinocidins against specific target pathogens.
© 2006 Elsevier B.V. All rights reserved.

Keywords: Antimicrobial; Peptide; Structure; Platelet; Kinocidin; Chemokine

1. Introduction

Antimicrobial peptides are typically small, cationic and amphipathic molecular effectors of innate immunity present in

organisms across the phylogenetic spectrum. Recently, a new group of antimicrobial peptides has been identified among classical cytokines: microbicidal chemokines [1–5]. Chemokines that exert direct microbicidal activity have been termed kinocidins [6,7]. Kinocidins are typically larger and have greater structural complexity than classical antimicrobial peptides. Moreover, distinct structural domains in kinocidins are hypothesized to confer complementary microbicidal and leukocyte-potentiating functions [7,8]. Thus, kinocidins represent multi-functional immune effector molecules that coordinate molecular and cellular host defense against infection.

Relative to most classical antimicrobial peptides, kinocidins have comparable antimicrobial spectra and efficacy [9,10]. Traditional antimicrobial peptides and kinocidins are also analogous in their rapid induction, mobilization, or accumulation in response to signals of infection [11–18]. However, in

contrast to classical antimicrobial peptides, the majority of which are confined within phagocytes or expressed on mucosa, kinocidins are commonly elaborated directly in the bloodstream. These considerations are consistent with the concept that kinocidins exert comparatively less host toxicity than many antimicrobial peptides [9,19]. Therefore, understanding critical structure–activity relationships in kinocidins will clarify their roles in host defense, and may assist in design of novel anti-infective therapeutics that are efficacious against increasingly antibiotic-resistant pathogens, and have minimal concomitant host cytotoxicity.

Recent studies offer general aspects of sequence and biochemical properties that may contribute to kinocidin antimicrobial efficacy [2,5–7,20]. However, specific structural determinants that confer their antibacterial versus antifungal properties, or their efficacies against strains differing in anti-microbial peptide susceptibility phenotypes, have not been defined. With these goals in mind, the current studies applied biochemical and biophysical techniques, integrated with quantitative molecular modeling, to uncover the principal determinants of antimicrobial activity in the PF-4 family of kinocidins.

2. Materials and methods

2.1. Microorganisms

Strain pairs of three prototypic human pathogens were used in this investigation: *Staphylococcus aureus* strains ISP479C and ISP479R (Gram-positive bacterium; [20]); *Salmonella typhimurium* strains 14028 and m5996s (Gram-negative bacterium; [21]); and *Candida albicans* strains 36082S and 36082R (fungus; [22]). Each of these well-characterized pairs have been used previously to evaluate antimicrobial peptide activity, and include isogenic counterparts that exhibit relative susceptible (S) or resistant (R) phenotypes to

one or more antimicrobial peptides. Organisms were cultured in brain heart infusion broth (BHI; Difco Laboratories, Detroit, MI; 37 °C with agitation) or yeast nitrogen broth (YNB; Difco; 30 °C with agitation) to logarithmic phase, and prepared as previously described [6]. In brief, cells were harvested by centrifugation, washed twice in appropriate assay buffer (below), sonicated briefly to ensure dispersion, and adjusted by optical density to desired inocula. Concentrations of final inocula were verified by quantitative culture.

2.2. Peptide synthesis

Previous studies have demonstrated that PMP-1 and hPF-4 contain three analogous structural domains [7]: (1) a relatively unstructured N-terminal domain containing the CXC motif characteristic of α-chemokines; (2) a highly α-helical and cationic C-terminal domain reflecting strong amphipathic propensity similar to many antimicrobial peptides; and (3) an interposing domain comprised of anti-parallel β-sheet domains, two of which constitute an iteration of the γ-core motif of cysteine-stabilized antimicrobial peptides [6]. A consensus peptide (cPMP) and its library were designed to reflect such structural domains in hPF-4, PMP-1, and variants thereof. A peptide library was synthesized to assess potential antimicrobial correlates associated with specific domains or broader regions in PF-4 family members (Table 1). In cPMP, residues were assigned to prioritize antimicrobial activity and increase the probability for molecular modeling (below) to reveal meaningful correlates of activity. The library was comprised of domains 15 amino acids in length, overlapping by 3 residues each, and larger peptides representing one-half of the full-length molecules (hemimers), encompassing the amino-(residues 1–37) and carboxy-terminal regions (residues 38–74; Fig. 1). A novel congener modeled to reflect key physicochemical properties of PF-4 family helical domains (RP-1; ALYK-KFKKKLLKSLKRLG; [23]) was also evaluated for efficacy in parallel to the above peptide panel. All peptides were synthesized by automated F-moc (9-fluorenyl-methyloxycarbonyl) chemistry. Classical antimicrobial peptides (human neutrophil defensin HNP-1; protamine; gramicidin D; Peptides International, Louisville, KY) were assayed as comparators.

2.3. Peptide purification and authentication

Native PMP-1 and synthetic cPMP walkthrough peptides were purified as previously described using reversed-phase HPLC [2]. Purified peptides were

Table 1
Comparative sequences of PF-4 family kinocidins, cPMP, and its peptide library

	N-terminal	Interposing	C-terminal
Principal structural domains in PF-4 kinocidins			
hPF-4	[1](A)EAEEDGDLQCLCVKTTSQVR	PRHITSLEVIKAGPHCPTAQLIATLKNGRKICLDL	QAPLYKKIIKKLLES[71]
hPF-4var	[1](A)EAEEDGDLQCLCVKTTSQVR	PRHITSLEVIKAGPHCPTAQLIATLKNGRKICLDL	QALLYKKIIKEHLES[71]
PMP-1	[1]SDDPKESEGDLHCVCVKTTSLVR	PRHITNLELIKAGGHCPTAQLIATLKNGRKLCLDP	QAALYKKVIKKLLKE[73]
AspPMP-1	[1]DDPKESEGDLHCVCVKTTSLVR	PRHITNLELIKAGGHCPTAQLIATLKNGRKLCLDP	QAALYKKVIKKLLKE[72]
PMP-1var1	[1]SDDPKESEGDLHCVCVKTTSLVR	PGHITNLELIKAGGHCPTANLIATKKNGRKLCLDL	QAALYKKIIKKLLES[74]
cPMP peptide library			
cPMP	[1]SDDPKESEGDLHCVCVKTTSLVR	PRHITNLELIKAGGHCPTANLIATKKNGRKLCLDL	QAALYKKIIKKLLES[74]
1–37	[1]SDDPKESEGDLHCVCVKTTSLVR	PRHITNLELIKAGG	
38–74		[38]HCPTANLIATKKNGRKLCLDL	QAALYKKIIKKLLES[74]
1–15	[1]SDDPKESEGDLHCVC[15]		
13–27	[13]CVCVKTTSLVRPRHI[27]		
25–39		[25]RHITNLELIKAGGHC[39]	
37–51		[37]GHCPTANLIATKKNG[51]	
49–63		[49]KNGRKLCLDL	QAALY[63]
60–74			[60]AALYKKIIKKLLES[74]

hPF-4 and PMP-1 are predominant antimicrobial peptide orthologues in rabbit and human platelets, respectively. Amino acid sequences for hPF-4 (GenBank Code gi|62739642), hPF-4var (GenBank Code, gi|130306), PMP-1 and its variant AspPMP-1 [GenBank Code gi|42411026; [7]] are available through the NCBI database. Sequences of PMP-1 variants were determined from multiple protein sequencing reactions (Yeaman et al., unpublished). As with human PF-4, the PMP-1 variants likely represent allelic polymorphisms. Principal structure domains are indicated for each full-length sequence, as well as the cPMP hemimer (1–37 and 38–74) and 15-mer peptide library. As detailed in the text, the N-terminal domains contain CXC chemokine motifs, the interposing regions contain a kinocidin iteration of the multidimensional γ-core signature present in a diverse range of cysteine-stabilized host defense peptides, and the C-terminal domains comprise a hallmark amphiphilic α-helical motif common to many classical antimicrobial peptides. Thus, cPMP represents a logical composite of the PF-4 family of kinocidin sequences.
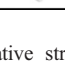
Domain	Model	Helix	Sheet	Turn	Other [a]
cPMP [b]		30.1	16.1	18.8	21.6
1-37		12.4	16.2	14.1	57.3
38-74		40.7	17.5	15.9	25.9
1-15		3.7	4.1	2.1	90.1
13-27		11.2	15.4	13.0	60.4
25-39		32.1	19.9	19.8	28.2
37-51		20.7	22.8	18.6	37.9
49-63		22.6	25.3	20.7	31.4
60-74		65.8	1.3	9.5	23.4

Fig. 1. Comparative structural features of cPMP and its library peptides. Secondary structure data were determined experimentally from independent CD spectra of each peptide as detailed in Materials and methods, and expressed as percent of structure. Data refer to corresponding hemimer or walkthrough domains, indicated in red to identify positioning within the full-length molecule. Cysteine bridges are indicated in yellow. Three-dimensional structures of full length and domain peptides were modeled as described previously [7]. A close agreement was identified between the modeled and experimentally-determined structural characteristics.

authenticated by matrix-assisted laser desorption ionization time-of-flight (MALDI-TOF; PerSeptive Biosystems, Foster City, CA) or electrospray (ES; Perkin-Elmer Corp., Boston, MA) spectrometry. Experimentally determined masses were within standard confidence intervals for calculated masses ($<\pm0.1\%$ or $<\pm0.04\%$ of peptide molecular weight for MALDI-TOF or ES mass spectrometry, respectively). Peptide composition and quantity were also verified by amino acid analyses (Molecular Structure Facility, University of California, Davis). PMP-1 was confirmed for expected antimicrobial activity by a standard radial diffusion assay [7], and all peptides were lyophilized and stored at −70 °C until use. Highly-purified human platelet factor-4 (hPF-4) was obtained commercially (Biosource International, Camarillo, CA) (Fig. 2).

2.4. Assays for antimicrobial efficacy

Complementary methods were used to assay antimicrobial efficacy of peptides in vitro against the panel of study strains.

2.4.1. Solid phase diffusion assay

A modified solid-phase diffusion assay [6] afforded specific advantages important to this study: (i) it allowed direct comparison of peptide activities versus distinct organisms; and (ii) it yielded continuous (non-quantal) data, facilitating computational modeling to examine structure-activity relationships. The assay media were buffered to pH 7.5 using PIPES (piperazine-*N,N'*-bis[2-ethanesulfonic acid] (Sigma). Following incubation at 37 °C (18 h for bacteria, 36 h for *C. albicans*), the diameter zones of inhibition surrounding wells were measured. All peptide antimicrobial assays were performed a minimum of three independent times.

2.4.2. Solution-phase assay

A solution-phase assay was also used to evaluate microbicidal efficacy of study peptides. Organisms were prepared as above in PIPES buffer, but lacking agarose. Peptides (range, 1.25–5 nmol/ml) were introduced into buffer containing organisms to achieve final inocula of 1×10^6 CFU/ml. Following

incubation for 1 h at 37 °C, aliquots were serially diluted and plated in triplicate for quantitative enumeration.

2.4.3. Biomatrix assay

Antimicrobial activities of cPMP$_{38-74}$ and cPMP$_{60-74}$ were assessed in human whole blood and homologous plasma and serum fractions as we have detailed previously [21]. The target strain of *Escherichia coli* is resistant to serum, ideal for use in assessing peptide antimicrobial activity in blood and blood-derived matrices [21]. Peptide (concentration range 1.0–50.0 µg/ml) was added either simultaneously with the microorganism (10 µl; 10^5 CFU/ml), or 2 h prior to the organism to achieve a pre-incubation period in the biomatrix. Mixtures were incubated with constant agitation for 2 h at 37 °C. After incubation, aliquots were diluted, quantitatively cultured in triplicate onto blood agar, and surviving organisms enumerated as CFU/ml. Experiments were performed a minimum of two independent times on different days and with different blood donor sources.

2.5. Spectrometric assessment of peptide structure

Secondary structures of cPMP library peptides were assessed by circular dichroism (CD) as previously detailed [22]. The CD spectra were deconvoluted into helix, β-sheet, turn, and extended structures using Selcon [23] accessed by on-line Dichroweb [24] interface (cryst.bbk.ac.uk/cdweb), and interpreted as previously described [22,25,26].

2.6. Computational modeling

To complement structure analyses, 3-D models of full-length cPMP and library peptides were created using complementary methods, as previously described [7]. In brief, homology techniques (SWISS-MODEL, BLASTP2) were
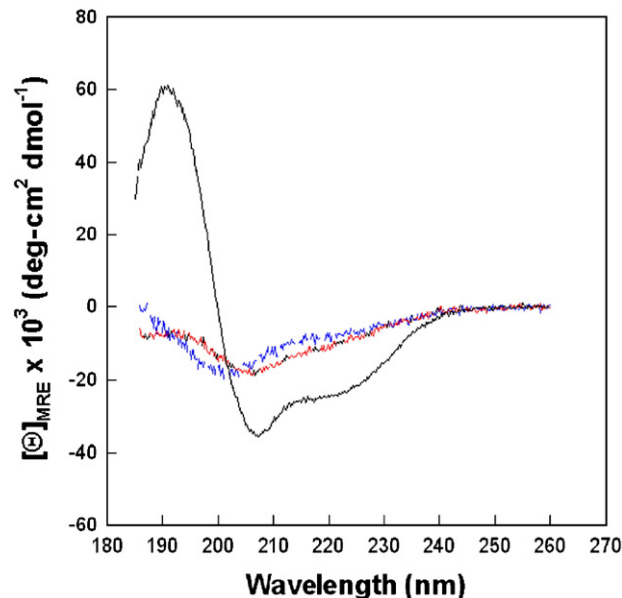
Fig. 2. Comparative circular dichroic spectra of antimicrobial cPMP domains 13–27 (red line), 49–63 (blue line), and 60–74 (black line). Note the double dichroic minima of domain 60–74 at 208 and 218 nm, corresponding to a highly ordered α-helical conformation. By comparison, domain 49–63 is considerably less helical, and contains substantially greater sheeting and turn propensity, reflecting its relative position within the greater topological configuration of the molecule. Domain 13–27 has more equivalent helical, sheeting, and turn propensities, with considerably more unstructured aspects. These comparisons illustrate the concept that, while all three domains have identical length and exhibit similar mass and net cationic charge, they have diverse secondary structure propensities that contribute to their distinct antimicrobial efficacies and spectra.

Table 2
Physicochemical profile of cPMP and library peptides

Domain	Physicochemical characteristics						
	Length	Mass [a]	pI [b]	Charge [c]	D_C [d]	M_H [e]	Hydropathy [f]
cPMP	74	8167	9.0	+6	+0.08	0.86	−16.42
1–37	37	4019	6.0	−1	−0.03	1.02	−13.42
38–74	37	4166	9.7	+7	+0.19	0.69	−2.38
1–15	15	1634	4.0	−4	−0.27	1.78	−11.82
13–27	15	1712	9.3	+3	+0.20	0.38	−0.59
25–39	15	1662	7.6	+1	+0.07	0.99	−2.9
37–51	15	1525	8.9	+2	+0.13	0.83	−0.62
49–63	15	1706	8.8	+2	+0.13	3.52	−2.55
60–74	15	1746	9.8	+4	+0.27	3.56	−3.42

Note the polarization of electrostatic charge and mass in the terminal domains. For example, despite being equal in residue number and similar in hydrophobic moment, the N-terminal domains 1–15 and C-terminal domains 60–74 have substantially different mass, as well as opposing charge, charge density, and hydropathy. With the exception of charge, large differences in these parameters among distinct domains are attenuated in context of their greater respective hemimer.

[a] Average mass (Da).

[b] Isoelectric point estimated in aqueous phase.

[c] Net charge as calculated at pH 7.

[d] Average charge density calculated as net charge [c]/number of residues (length).

[e] Mean hydrophobic moment.

[f] Partition coefficient hydropathy (hydrophobic potential as implemented in HINT).

used for combinatorial extension alignments and to search for primary sequence similarities in the ExNRL-3D database [27,28]. In parallel, the SIM alignment algorithm [29] prioritized templates with greatest sequence identity. ProModII was used to conduct primary and refined match analyses. In a complementary strategy, amino acid sequences were converted to putative solution conformations by sequence homology [Composer; [30]] and threading methods [Matchmaker [31], Gene-Fold [32]] implemented with SYBYL software (Tripos Associates, St. Louis, MO). Conformers of target peptides were refined using the AMBER95 force field and molecular dynamics [33]. Preferred conformations were determined from extended molecular dynamics, with torsion angles of peptide bonds adjusted to 180 ± 15 degrees with minimal constraints (0.4 kJ). The specific physicochemical properties of peptides were visualized by MOLCAD [34] and HINT [35], superimposed upon backbone trajectories or projected onto water-accessible molecular surfaces. Molecular dynamics were executed without constraints, or with the α-helical region constrained by applying a 0.4 kJ penalty to canonical Ramachandran ϕ and ψ angles. Global energy was minimized after removal of constraints and aggregates. Model conformations were prioritized based on integrated criteria as appropriate: (i) favorable strain energy (molecular mechanics); (ii) empirical positional (pseudo) energy functions; and (iii) preservation of spatial conservation of cysteine pairs [7].

2.7. Statistical evaluation

Differences in results of independent assays of strain peptide susceptibility were analyzed using the Wilcoxon Rank Sum test with Bonferroni correction for multiple comparisons. Linear correlation coefficients (r^2) were determined with the statistical package KYPlot (version 2.0).

3. Results

3.1. Peptide library

Comparative sequences of PF-4 family members, cPMP, and its library peptides are summarized in Table 1. Native and synthetic peptides were purified to >95% homogeneity by RP-HPLC (data not shown), and authenticated to have masses within ±0.1% of calculated values (Table 2).

Table 3
Comparative antimicrobial efficacies of PMP-1, hPF-4, and the cPMP library peptides

	Organism	*S. aureus* [a]		*S. typhimurium* [b]		*C. albicans* [c]	
	Strain	ISP479C	ISP479R	5996s	14028	36082S	36082R
	Peptide	Zone of inhibition (mm)					
	PMP-1	6.5	3.5	8.5	4.5	4.0	2.5
	hPF-4	5.5	3.5	7.0	5.0	3.5	2.0
Hemimers	1–37	0.5 [d]	0.5	1.5	0.5	0.5	0.5
	38–74	6.2	5.0	9.3	5.4	5.0	4.1
Walkthrough domains	1–15	0.5	0.5	0.5	0.5	0.5	0.5
	13–27	0.9	1.1	7.2	2.4	2.6	1.6
	25–39	0.5	0.5	0.9	0.5	0.8	0.5
	37–51	0.5	0.5	0.5	0.5	0.5	0.5
	49–63	2.8	1.9	8.8	4.0	5.3	5.7
	60–74	5.6	2.9	8.8	5.5	5.1	4.6
Novel agent	RP-1	6.0	5.0	6.0	6.0	3.0	4.0
Classical peptides	HNP-1	6.5	ND [e]	5.3	ND	5.5	5.3
	Protamine	7.5	7.5	5.5	5.8	12.8	6.3
	Gramicidin D	7.8	7.0	2.3	2.0	0.5	2.5

Note a predominance of broad spectrum antimicrobial efficacy corresponding to the C-terminal hemimer (38–74) and its subdomains (49–63 and 60–74). Interestingly, specific activity versus *S. typhimurium* corresponds to the more N-terminal proximate domain 13–27. However, the efficacy of this latter domain is largely mitigated in context of its N-terminal hemimer (1–37).

Mean data from a minimum of 2 experiments performed independently with reproducible results (standard error of the mean<5%).

[a] *S. aureus* pair: ISP479C (peptide-susceptible; C) and ISP479R (-resistant; R).

[b] *S. typhimurium* pair: 5996s (peptide-susceptible; s) and 14028 (-resistant).

[c] *C. albicans* pair: 36082S (peptide-susceptible; S) and 36082R (-resistant; R).

[d] Limit of detection, 0.5 mm.

[e] ND, not determined.

3.2. Biochemical assessment of molecular domains

The amino acid compositions and overall biochemical attributes of hPF-4 and PMP-1 have been compared previously [7]. The relative biochemical features of cPMP and its library peptides are summarized in Table 2. Molecular masses of the hemimers were comparable (4019 Da [N-terminal 1–37] versus 4166 Da [C-terminal]), as were masses of individual walk-through 15-mer peptides (range, 1525 Da [37–51] to 1746 Da [60–74]). In contrast, electrostatic charge, steric bulk, and hydropathy varied among structural domains, and corresponded to native molecules. Consistent with this concept, greatest cationic charge density and pI localized to the C-terminal hemimer, and specifically to the C-terminal domain spanning residues 60–74 (net charge at pH 7, +4; Table 2). On the contrary, the greatest anionic density and lowest pI polarized to the N-terminal hemimer, and particularly to the N-terminal domain consisting of residues 1–15 (net charge at pH 7, −4; Table 2). Although no clear trends in hydropathy were detected, the most terminal domains (e.g., N-terminal residues 1–15, and C-terminal residues 49–63, 60–74) exhibited greatest hydrophobic moments, suggesting they represent the most amphipathic regions of hPF-4 and PMP-1 (Table 2).

3.3. Structural assessment of molecular domains

CD spectrometry was utilized to assess secondary structure in cPMP walkthrough peptide and hemimer domains (Fig. 1). These structures were compared to that of human PF-4, or PMP-1, previously determined by NMR or X-ray spectrometry [36] or homology modeling [7]. As anticipated, general secondary structure themes of cPMP peptide domains reflected corresponding regions within native PMP-1 and hPF-4. Such themes included a relatively extended N-terminal domain (circa residues 1–23), an interposing anti-parallel β-sheet hairpin domain (circa residues 24–59), and a C-terminal α-helical domain (circa residues 60–74). These findings suggest that walkthrough peptides and cPMP hemimers retained secondary structural elements of cognate domains previously identified in full-length PMP-1 [7] and hPF-4 [36].

3.4. Antimicrobial efficacy of molecular domains

The antimicrobial efficacies of study peptides versus a panel of well-characterized Gram-negative, Gram-positive and fungal organisms are summarized in Table 3. Consistent with our prior observations [2,10,37,38], native PMP-1 and hPF-4 molecules exerted equivalent antimicrobial spectra and efficacies. Importantly, several functional themes emerged from studies of the cPMP peptide library in comparison to these molecules. First, the antimicrobial efficacies of study peptides in radial diffusion assay were generally greatest against Gram-negative target organisms (*S. typhimurium*). Second, in most cases, PMP-1, hPF-4, or cPMP peptides exerted efficacies corresponding to established peptide-susceptible or -resistance phenotypes, with greater efficacies versus the former group. Third, in the cPMP library, the strongest antimicrobial efficacy localized to the C-

terminal hemimer (residues cPMP$_{38-74}$), and C-terminal domains 49–63 and 60–74 thereof, representing the corresponding regions of PMP-1 and hPF-4 [7]. For example, domains cPMP$_{49-63}$ and cPMP$_{60-74}$ had greater efficacy versus either *C. albicans* strain than did the parent molecule, and particularly so against the peptide-resistant strain. Interestingly, a novel antimicrobial domain, cPMP$_{13-27}$, was localized to the N-terminal aspect of cPMP. Its antimicrobial efficacy was greatest versus *S. typhimurium*, more modest versus *C. albicans*, and minimal versus *S. aureus* (Table 3). However, the N-terminal hemimer (cPMP$_{1-37}$) encompassing domain cPMP$_{13-27}$ was devoid of detectable antimicrobial activity against any organism assayed. Likewise, no antimicrobial efficacy was detected against study organisms in N-terminal domain 1–15, or interposing domains 25–39 or 37–51 (Table 3). Complementing the above findings, solution-phase data revealed highly potent efficacies of the cPMP$_{38-74}$ at concentrations descending to 1.25 nmol/ml (Fig. 3). In most cases, cPMP antimicrobial domains compared favorably in efficacy to classical peptides, and paralleled those of the peptide mimetic, RP-1.

The physiological relevance of observed antimicrobial activities of (cPMP$_{38-74}$) and (cPMP$_{60-74}$) were assessed in the *ex vivo* biomatrix assay. Importantly, cPMP$_{38-74}$ demonstrated significant efficacy in blood matrices, causing decreases of up to
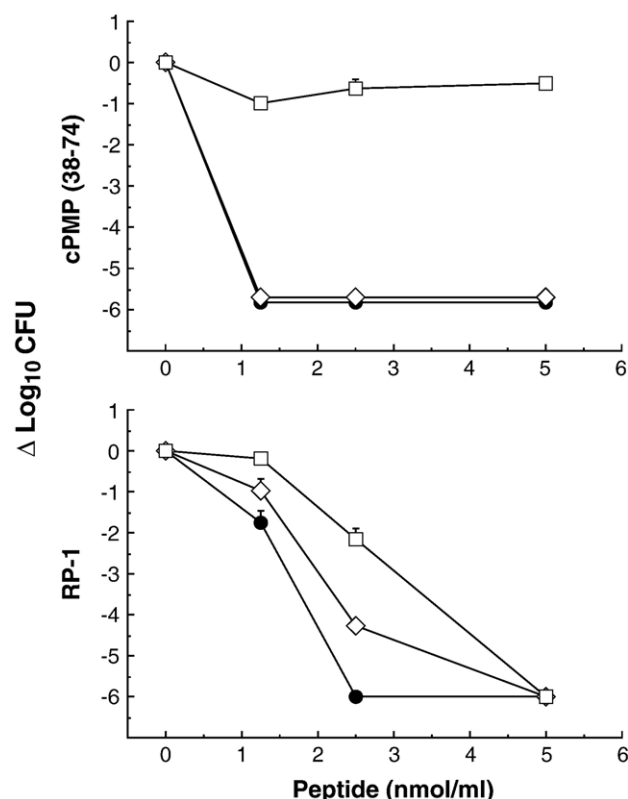
Fig. 3. Solution-phase microbicidal activities of cPMP$_{38-74}$ and RP-1. One million CFU of the indicated microorganism per milliliter were incubated with peptide (range, 1.25–5.0 nmol/ml) in PIPES (10.0 mM, pH 7.5) for 1 h at 37 °C. Surviving CFU were enumerated and indicated as change from the initial log$_{10}$ CFU. ◊, *S. aureus* ATCC 27217; ●, *S. typhimurium* strain 5996s; □, *C. albicans* ATCC 36082. Data are means±SD (minimum *n*=2).

log 5 CFU/ml at 10 µg/ml peptide (Fig. 4). Likewise, cPMP$_{60-74}$ was also highly efficacious in this assay, with a 5 log reduction in CFU/ml in serum at peptide concentrations as low as 25 µg/ml. Greatest efficacy was seen in whole blood and serum in co-incubation studies, with less activity in plasma fractions or after 2 h pre-incubation.

3.5. Structural correlates of antimicrobial efficacy

Polypeptide composition, sequence, and secondary structure predictions were compared with antimicrobial efficacy to identify putative functional correlates of cPMP peptide domains.
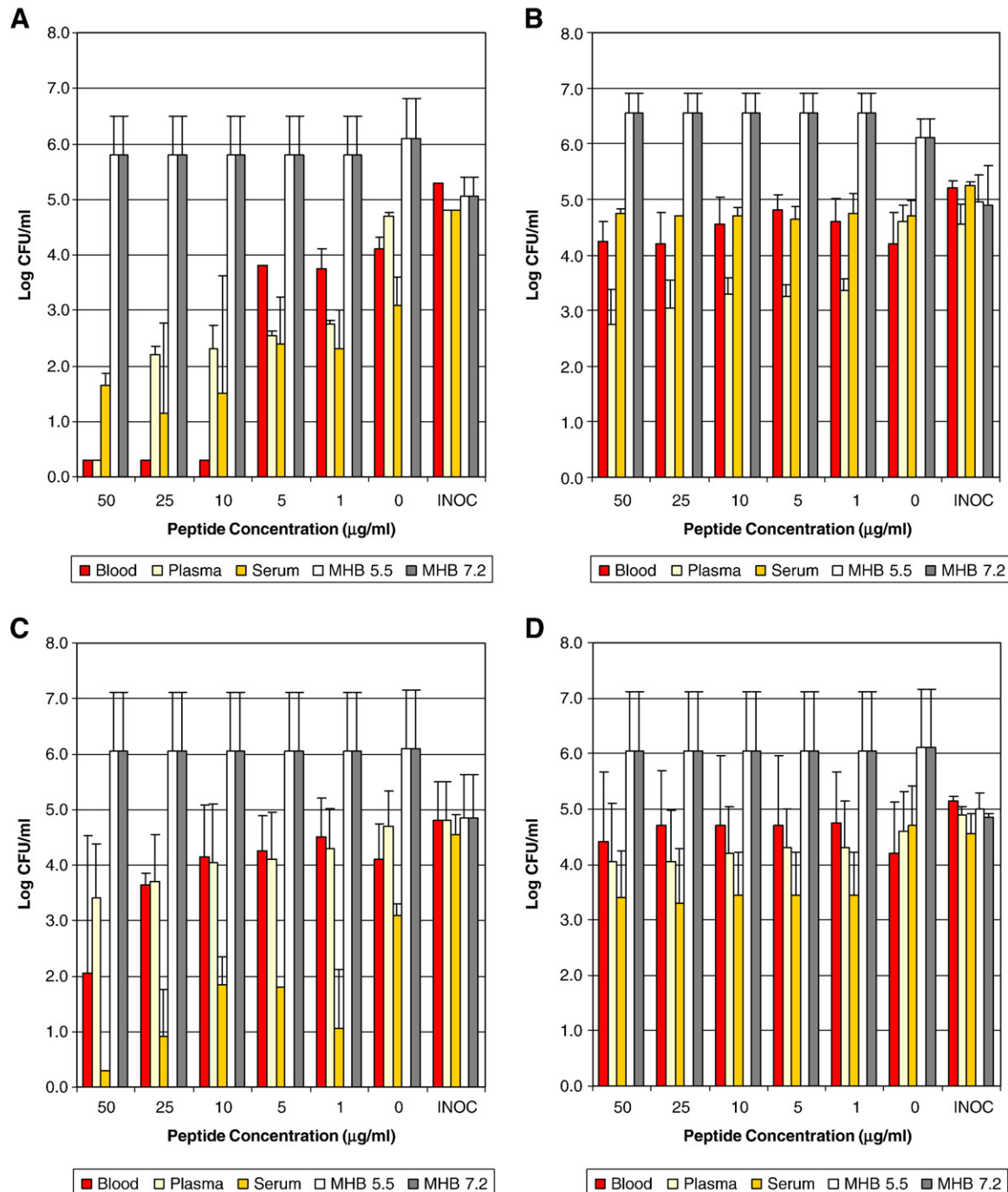

Fig. 4. Antimicrobial efficacy of cPMP modular domains in human blood matrices. The cPMP$_{38-74}$ (γ-core+ α-helix; [20,62]) or cPMP$_{60-74}$ (α-helix) domains were assayed in human blood, plasma, and serum as compared with artificial media (MHB) at pH 5.5 and 7.2. (A) efficacy of cPMP$_{38-74}$ in simultaneous co-incubation with target organisms; (B) efficacy of cPMP$_{38-74}$ pre-incubated in biomatrices or media (2 h, 37 °C) prior to introduction of the organism; (C) efficacy of cPMP$_{60-74}$ in simultaneous co-incubation with the organism; (D) efficacy of cPMP$_{60-74}$ pre-incubated in biomatrices or media prior to introduction of the organism. Initial *E. coli* inocula (INOC) were 10^5 CFU/ml, and the sensitivity of detection considered to be 0.3 log10 CFU/ml. Notably, cPMP$_{38-74}$ exhibited greater efficacy than cPMP$_{60-74}$ in whole blood and plasma matrices, particularly on co-incubation with target organisms. This finding supports the hypothesis that γ-core motifs may facilitate microbicidal functions of distinct structural domains (e.g., the microbicidal α-helix or cPMP$_{60-74}$) in relevant contexts of infection [8,20,62].

3.5.1. Physicochemical correlates of peptide antimicrobial efficacy

Linear regression analyses revealed direct and inverse relationships between independent physicochemical parameters and antimicrobial efficacy (Table 4). Significant direct ($r^2 > 0.5$) correlations were identified associating net cationic charge and efficacy versus all organisms tested. However, charge density of a given domain did not achieve significant correlation with antimicrobial efficacy. Notably, while helical propensity correlated with efficacy against peptide-susceptible and -resistant *S. aureus*, this parameter only correlated with efficacy against peptide-resistant strains of *S. typhimurium* or *C. albicans*. In contrast, increasing hydrophobic moment, sheeting, and turn propensities yielded significant inverse ($r^2 < 0.05$) correlates of antimicrobial efficacy versus all study organisms (Table 4). Peptide length, mass, or hydropathy emerged as being inversely correlated with efficacy solely versus peptide-resistant counterparts of distinct pathogens (Table 4).

3.5.2. Mapping antimicrobial determinants in cPMP

Glycine scanning enabled localization of charged residues or groups of residues correlating with efficacy versus peptide-susceptible or -resistant target organisms (Fig. 5). Notably, particular charged residues correlated significantly with antimicrobial efficacy. Although these individual residues are distributed throughout the molecule, certain amino acid moieties appeared to be coordinated in 3-dimensional space as governed by secondary structure. For example, anionic charge clustering at the N-terminus, and cationic charge concentrated to the C-terminus and apices of the γ-core motif in hPF-4 and PMP-1, correlate to efficacy versus peptide-resistant *S. typhimurium*

strain 14028R (Fig. 5). In this case, efficacy correlated with cationic charge concentrated by relatively close proximity of residues K17, K34, and K64. Conversely, diminishing anionic potential at positions E31 and D57 also correlated with efficacy. In contrast to conventional paradigms, increasing anionic charge localized to residue E73 at the penultimate aspect of the helical domain also contributed to efficacy against each organism studied. With few exceptions, correlates of electrostatic position and efficacy versus susceptible- or resistant-strains were similar for all organisms tested (Fig. 5).

4. Discussion

4.1. Structural themes of antimicrobial activity in PF-4 kinocidins

Analysis of antimicrobial determinants in hPF-4, PMP-1, and other PF-4 family kinocidins reveals recurring themes of structure and activity in these multifunctional host defense molecules (Fig. 6).

4.2. Physicochemical correlates of antimicrobial efficacy

The physicochemical properties and secondary structural features of specific cPMP domains yielded insights into the antimicrobial determinants of PF-4 kinocidins. For example, domain cPMP$_{13-27}$ is proximate to the N-terminus, has a net charge of +3, and an extended secondary structure. These features correlate predominantly to efficacy versus *S. typhimurium*, but little or no activity against *C. albicans* or *S. aureus*. However, in context of the larger N-terminal hemimer (residues 1–37), cPMP$_{13-27}$ is charge-neutralized, and its antimicrobial activity abrogated. Domain cPMP$_{49-63}$ also has a net cationic charge (+2), but localizes near the C-terminus, and has helical and sheet propensity. Because its charge is similar to domain 13–27, anti-candidal and anti-staphylococcal efficacies of domain 49–63 likely integrate secondary structure. The cPMP$_{60-74}$ domain illustrates a distinct structure–function theme. Its cationic charge and amphipathic nature were associated with greater efficacy versus *S. aureus* as compared with domains 13–27 or 49–63. Furthermore, domains cPMP$_{49-63}$ and cPMP$_{60-74}$ retained antimicrobial efficacy within the context of the C-terminal hemimer (residues 38–74). Likewise, direct antimicrobial activity has been associated with α-helices in other microbicidal chemokines [20,21,39,40]. Similar structure–function correlates have been identified by Lejon and colleagues for pentadecapeptide congeners derived from lactoferrin [41].

A particularly important aspect of this study was to demonstrate antimicrobial efficacy of the C-terminal hemimer (cPMP$_{38-74}$) and helix (cPMP$_{60-74}$) regions in relevant biological contexts of human blood and blood-derived matrices. In these physiologically complex settings, these polypeptides had considerable efficacy against *E. coli* ML-35 at concentrations descending to 10 μg/ml. This finding was significant for several reasons. First, it substantiates the

Table 4
Univariate analysis of structure–activity relationships in cPMP library peptides

Organism	*S. aureus*[a]		*S. typhimurium*[b]		*C. albicans*[c]	
Strain	ISP479C	ISP479R	5996s	14028	36082S	36082R
Property	Linear correlation coefficient (r^2)					
Length	0.23	0.28	0.22	0.05	0.26	0.08
Mass	0.25	0.30	0.24	0.06	0.28	0.10
pI	0.44	0.34	0.48	0.48	0.49	0.54
Charge	0.66	0.67	0.67	0.58	0.70	0.63
D_C	0.35	0.25	0.33	0.44	0.34	0.45
M_H	<0.01	<0.01	0.06	<0.01	0.02	0.04
Hydropathy	0.13	0.03	0.27	0.19	0.30	0.31
Helix	0.56	0.53	0.20	0.64	0.18	0.64
Sheet	0.09	0.06	0.01	0.09	0.01	0.01
Turn	<0.01	<0.01	0.09	<0.01	0.03	0.02

Significant direct (*) correlations ($r_2 > 0.5$) are indicated by black text on gray shading, and significant inverse (+) correlations ($r_2 < 0.05$) are indicated by white text on black shading. Note that charge is a uniform direct correlate of efficacy, while M_H, sheeting, and turn propensity are uniform inverse correlates of efficacy among these peptides. Interesting, some parameters emerged as specific correlates of efficacy versus some organisms but not others. For example, helical propensity corresponds to efficacy against both *S. aureus* strains, but only peptide-resistant counterparts in *S. typhimurium* or *C. albicans*.

[a]*Staphylococcus aureus* strain pair as detailed in the legend of Table 3.
[b]*Salmonella typhimurium* strain pair as detailed in the legend of Table 3.
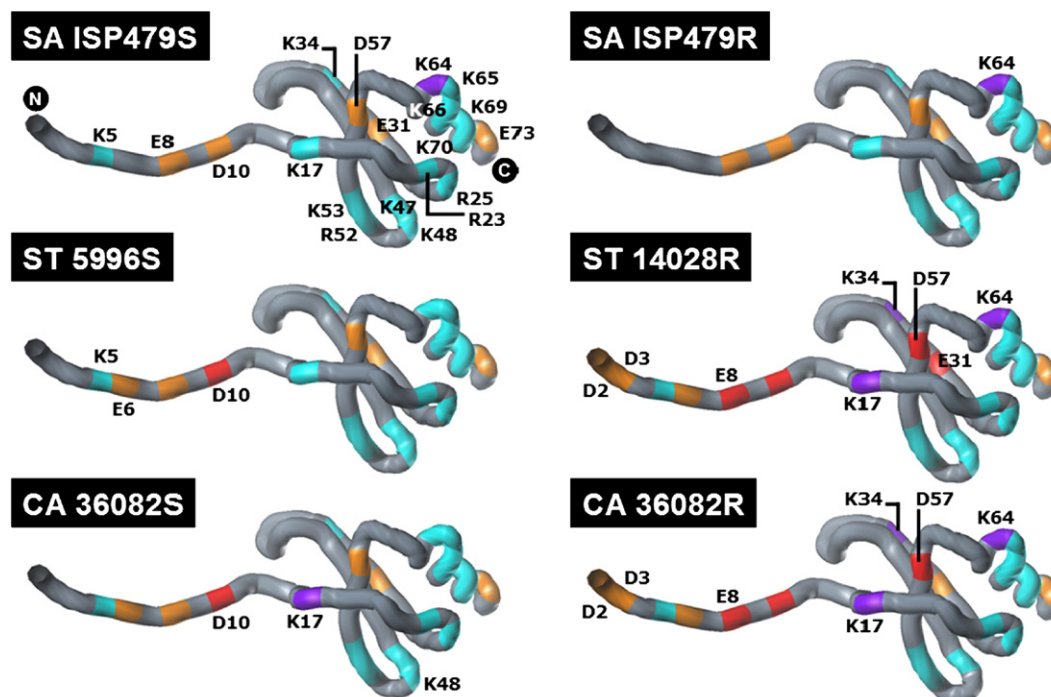[c]*Candida albicans* strain pair as detailed in the legend of Table 3.

Fig. 5. Positional amino acid residue correlates of antimicrobial efficacy. In these studies, 74 mutant peptides substituting glycine at successive positions along the cPMP sequence were evaluated *in silico* for efficacy as compared to the parent molecule. For each organism, parental versus mutant residues are then classified relative to their contribution to efficacy (relative efficacy ratio [RER]), and highlighted per the following color schema: purple, strong cationic contribution (1.079 to 1.12); cyan, modest cationic contribution (1.037 to 1.078); orange, modest anionic contribution (0.9192 to 0.8175); red, strong anionic contribution (0.8714 to 0.83); gray, no significant correlate of efficacy (0.9957 to 1.037). Respective amino- and carboxy-termini are indicated as N and C. The RER for correlates of efficacy are indicated in parentheses. These experiments reveal residues that are integral to antimicrobial efficacy against a specific organism, between susceptible or resistant strains, and between different organisms. For clarity, residues contributing significant correlates of efficacy are labeled in the first panel; thereafter, only residues with distinct impact on efficacy between respective peptide-susceptible and-resistant strains are indicated.

concept that kinocidins or microbicidal fragments thereof have antimicrobial efficacy in relevant and non-austere conditions. Second, cPMP$_{38-74}$ and cPMP$_{60-74}$ exhibited significant efficacy in serum fractions on co-incubation, and retained activity in serum even after 2 h of pre-incubation before addition of the target pathogen. Prior studies with other antimicrobial peptides suggest most are substantially reduced in efficacy or inactivated in serum [42,43], possibly corresponding to their generally poor efficacy in animal models of hematogenous infection. One potential challenge to furthering the current line of investigation will be to identify optimal experimental models that permit detection of antimicrobial activity in vivo. Nonetheless, the present data are an extremely important step toward demonstrating the likelihood that cPMP and related kinocidins or host defense peptides have unambiguous antimicrobial roles in relevant contexts in vivo [6,7,20].

4.3. Topographical correlates of antimicrobial efficacy

The above data highlight that antimicrobial efficacy of polytopic PF-4 or other kinocidins derives from a combination of independent and collective factors, including charge, steric bulk and other features. An important aspect of the current investigation was to gain insight into potential holistic or autonomous correlates of antimicrobial efficacy in PF-4

kinocidins. The present data show that autonomous domains of these molecules (e.g., the α-helical domain) are capable of retaining antimicrobial function reflecting their full-length precursors. Thus, structural contributions to antimicrobial efficacy and spectra may rely on individual domains. However, such function may also derive from cooperativity among such discrete domains in the context of the greater molecule. Differential antimicrobial efficacies of library peptides also substantiate roles for distinct spatial arrangements of charge and steric bulk among functional domains. For example, helical propensity influences amphipathicity and polar angle, and is characteristic of classic helical antimicrobial peptides [12–15]. Moreover, polarization of charged residues to the poles of the hemimer 38–74 is consistent with the pattern of cationic distribution in γ-core signatures of classical antimicrobial peptides [6]. This hemimer exerted the greatest efficacy and spectrum of any peptide tested, with significant activities against isogenic peptide-susceptible and -resistant strains. It should be recognized that electrostatic forces have relatively long-range influences, with energies inversely related to distance. This fact reinforces the findings that antimicrobial activity of one domain can be significantly influenced by surrounding molecular context. An excellent example of this phenomenon is illustrated in comparing antimicrobial profiles of the N-terminal cPMP$_{1-37}$ hemimer with its subdomain cPMP$_{13-27}$. Efficacy of the latter peptide is abrogated in context of the hemimer. An opposite
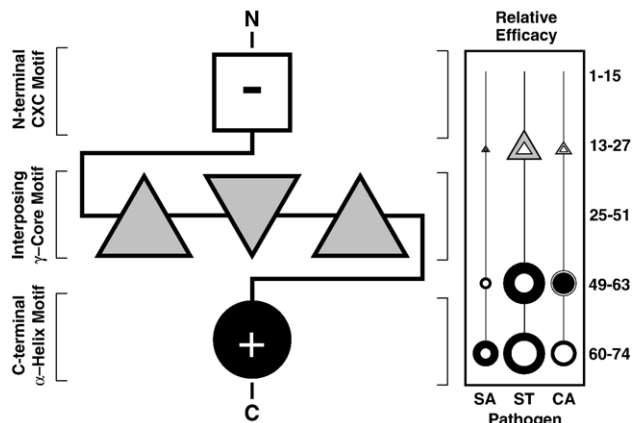
Fig. 6. Integrative functional topology model of PF-4 family kinocidins. Structural domains are represented in topological format: □, extended/turn domain; △, β-sheet domain; and ●, α-helical domain. The CXC, γ-core, and amphipathic helical motifs are unique to their respective N-terminal, interposing, and C-terminal domains. Note how the net electrostatic charge is polarized to termini in the primary structure: the extended and electronegative N-terminus is isolated from the highly structured and electropositive C-terminal helix by the interposing anti-parallel β-sheet region. These features illustrate the modular configurations of PF-4 and related kinocidins. The iconogram depicts the comparative sequence domains and topology corresponding to efficacy versus specific pathogens. Relative efficacies of walkthrough peptides versus bacterial (Gram-positive *S. aureus* [SA] or Gram-negative *S. typhimurium* [ST]) or fungal pathogens (*C. albicans* [CA]) assayed are indicated by proportionate area. Filled or shaded topological icons correspond to efficacy versus peptide-susceptible strains, and open icons correspond to efficacy versus orthologous peptide-resistant strains. Note the bimodal correlates of topology and efficacy, particularly versus *S. typhimurium*. For illustrative purposes, the non-antimicrobial domains 25–39 and 37–51 have been combined as 25–51 in this figure.

effect was observed in the C-terminal hemimer, where efficacy of the cationic and α-helical cPMP$_{60-74}$ appeared to be augmented in context of antimicrobial contributions by the C-terminal aspect of its γ-core motif. Thus, the antimicrobial and chemokine functions of kinocidins are likely conferred by discrete structural domains as configured to the γ-core motif [44,45].

4.4. Modular topology of antimicrobial determinants in PF-4 kinocidins

The segregation of functional modules (e.g., extended N-terminal chemotactic domain versus the C-terminal α-helix) supports the hypothesis that kinocidins may disassemble into autonomous and complementary effectors in response to stimuli (e.g., proteases) in contexts of infection [8]. Examples of proteolytic processing of kinocidins and classical antimicrobial peptides include the generation of N-terminal variants of PMP-1 [7], PBP cleavage into consecutive CTAP-3, β-TG, and NAP-2 peptides [2,4], and removal of charge-neutralizing pre–pro- or pro-piece sequences in defensins [46,47].

The current studies provide evidence that cPMP$_{60-74}$ can act independently of the parent molecule, retaining microbicidal efficacy in vitro and in complex blood and blood-derived matrices. Whether this domain is liberated *in vivo* is not known, however several intriguing observations lend support to this

hypothesis. First, the α-helical domain of PMP-1 is routinely liberated and can be isolated from the parent molecule in supernatants of thrombin-stimulated platelets (Yeaman et al., unpublished). The α-helical domain of PMP-1 and hPF-4 appears to be highly accessible to proteases, whether in monomeric or multimeric configurations common for this family [36]. In the monomer, the C-terminal α-helical domain is tethered to the remainder of the molecule by an exposed linking region. In the tetrameric configuration, the helical domains are on the solvent exposed outermost facets of the multimer. Likewise, recent studies by Braff and colleagues [48] are consistent with this paradigm, as are reports of antimicrobial constituents embedded in larger precursor proteins [40,49,50]. Taken together, such observations imply that the α-helical domain would be accessible and would likely retain its antimicrobial properties if liberated from the holoprotein.

One finding of particular interest is the marked biophysical similarity between the α-helical cPMP$_{60-74}$ domain and many classical antimicrobial peptides. This fragment is most similar to the magainin peptides with respect to length, helicity, cationicity, and amphipathicity; cPMP$_{60-74}$ is less similar to LL-37 and the cecropins, which are considerably larger [51]. Based on such parallels, we predicted significant antimicrobial efficacy would be associated with this domain. Importantly, the mechanism by which such α-helical peptides interact with disrupt biological membranes has been the subject of many excellent studies [52–57]. Indeed, recent studies have demonstrated that a synthetic peptide modeled on the cPMP helix recapitulates the antimicrobial efficacy and mechanism of it native template [58].

4.5. Insights into mechanisms of kinocidin antimicrobial action and resistance

The current studies also provide insights into the mechanisms of PF-4 family or other kinocidin antimicrobial action and resistance. Interestingly, the current data differentiate net charge from charge density as a correlate of antimicrobial efficacy. Further, several significant correlates of efficacy corresponded to groups of ionic amino acids. It follows that pathogens use various mechanisms to increase the net cationic charge of the cell envelope, thereby reducing affinity and in turn, increasing resistance to cationic peptides [59,60]. It should be noted, that although current studies emphasize charge correlates of efficacy, the potential importance of other physicochemical parameters (e.g., bulk, hydrophobicity) and conformation to antimicrobial efficacy should not be underestimated. Thus, while charge may be critical to initiate interactions between peptide and target membrane, global biophysical features may be essential for subsequent mechanisms of peptide microbicidal activity.

An intriguing observation was that differences in peptide efficacy were generally greater between peptide-resistant and -susceptible pairs of the same species, than among -susceptible phenotypes of different species. This finding suggests that specific peptides exert somewhat different mechanisms of action against specific organisms, or that distinct organisms employ different modes of resisting a given peptide. For example, in *S. aureus*, decreased charge in the N-terminal

hemimer correlated with increased resistance. In contrast, charged residues in the C-terminal domain were found to be equally important versus peptide-susceptible and -resistant *S. aureus* strains. By comparison, a reduction in charge near the cationic poles of the γ-core (e.g., K48 and K64 in cPMP) corresponds to peptide-resistance in *C. albicans*.

Finally, we recognize the limits of the current investigations. Using the same basis sets that yielded robust biophysical correlates of peptide antimicrobial efficacy, we did not identify correlations between changes in antimicrobial efficacy and (1) hydrophobic properties or (2) hydrogen bonding potential. Such a result should not be interpreted to mean these factors are irrelevant to antimicrobial efficacy [31–33,61,62]. Complex relationships in peptide structure and antimicrobial activity will benefit from resolution by increasingly fine-grained basis sets. Thus, the current studies offer novel insights into the molecular effectors of host defense, and hold promise for discovery, design, and development of novel anti-infective agents that are efficacious against pathogens are increasingly refractory to conventional therapies.

Acknowledgments

References

[1] M.R. Yeaman, The role of platelets in antimicrobial host defense, Clin. Infect. Dis. 25 (1997) 951–968 (quiz 969–970).

[2] Y.Q. Tang, M.R. Yeaman, M.E. Selsted, Antimicrobial peptides from human platelets, Infect. Immun. 70 (2002) 6524–6533.

[3] A.M. Cole, T. Ganz, A.M. Liese, M.D. Burdick, L. Liu, R.M. Strieter, Cutting edge: IFN-inducible ELR-CXC chemokines display defensin-like antimicrobial activity, J. Immunol. 167 (2001) 623–627.

[4] J. Krijgsveld, S.A. Zaat, J. Meeldijk, P.A. van Veelen, G. Fang, B. Poolman, E. Brandt, J.E. Ehlert, A.J. Kuijpers, G.H. Engbers, J. Feijen, J. Dankert, Thrombocidins, microbicidal proteins from human blood platelets, are C-terminal deletion products of CXC chemokines, J. Biol. Chem. 275 (2000) 20374–20381.

[5] D. Yang, Q. Chen, D.M. Hoover, P. Staley, K.D. Tucker, J. Lubkowski, J.J. Oppenheim, Many chemokines including CCL20/MIP-3alpha display antimicrobial activity, J. Leukoc. Biol. 74 (2003) 448–455.

[6] N.Y. Yount, M.R. Yeaman, Multidimensional signatures in antimicrobial peptides, Proc. Nat. Acad. Sci. U. S. A. 101 (2004) 7363–7368.

[7] N.Y. Yount, K.D. Gank, Y.Q. Xiong, A.S. Bayer, T. Pender, W.H. Welch, M.R. Yeaman, Platelet microbicidal protein 1: structural themes of a multifunctional antimicrobial peptide, Antimicrob. Agents Chemother. 48 (2004) 4395–4404.

[8] M.R. Yeaman, N. Yount, Code among chaos: immunorelativity and the AEGIS model of antimicrobial peptides, ASM News 71 (2005) 21–27.

[9] M.R. Yeaman, A.S. Bayer, S.P. Koo, W. Foss, P.M. Sullam, Platelet microbicidal proteins and neutrophil defensin disrupt the *Staphylococcus aureus* cytoplasmic membrane by distinct mechanisms of action, J. Clin. Invest. 101 (1998) 178–187.

[10] M.R. Yeaman, Y.Q. Tang, A.J. Shen, A.S. Bayer, M.E. Selsted, Purification and in vitro activities of rabbit platelet microbicidal proteins, Infect. Immun. 65 (1997) 1023–1031.

[11] R.I. Lehrer, T. Ganz, Defensins of vertebrate animals, Curr. Opin. Immunol. 14 (2002) 96–102.

[12] M. Zasloff, Antimicrobial peptides of multicellular organisms, Nature 415 (2002) 389–395.

[13] H.G. Boman, Antibacterial peptides: basic facts and emerging concepts, J. Intern. Med. 254 (2003) 197–215.

[14] S. Tauszig, E. Jouanguy, J.A. Hoffmann, J.L. Imler, Toll-related receptors and the control of antimicrobial peptide expression in *Drosophila*, Proc. Natl. Acad. Sci. U. S. A. 97 (2000) 10520–10525.

[15] J.P. Powers, R.E. Hancock, The relationship between peptide structure and antibacterial activity, Peptides 24 (2003) 1681–1691.

[16] R. Lorenz, M. Brauer, Platelet factor 4 (PF4) in septicaemia, Infection 16 (1988) 273–276.

[17] S. Mezzano, M.E. Burgos, L. Ardiles, F. Olavarria, M. Concha, I. Caorsi, E. Aranda, D. Mezzano, Glomerular localization of platelet factor 4 in streptococcal nephritis, Nephron 61 (1992) 58–63.

[18] Y. Yamamoto, T.W. Klein, H. Friedman, Involvement of mannose receptor in cytokine interleukin-1beta (IL-1beta), IL-6, and granulocyte-macro-phage colony-stimulating factor responses, but not in chemokine macrophage inflammatory protein 1beta (MIP-1beta), MIP-2, and KC responses, caused by attachment of *Candida albicans* to macrophages, Infect. Immun. 65 (1997) 1077–1082.

[19] M.R. Yeaman, A.S. Ibrahim, J.A. Ritchie, S.G. Filler, A.S. Bayer, J.E. Edwards Jr., M.A. Ghannoum. Infectious Disease Society of America Abstract 491 (1995).

[20] N.Y. Yount, M.R. Yeaman, Structural congruence among membrane-active host defense polypeptides of diverse phylogeny, Biochim. Biophys. Acta 1758 (2006) 1373–1386.

[21] M.R. Yeaman, K.D. Gank, A.S. Bayer, E.P. Brass, Synthetic peptides that exert antimicrobial activities in whole blood and blood-derived matrices, Antimicrob. Agents Chemother. 46 (2002) 3883–3891.

[22] D.C. Sheppard, M.R. Yeaman, W.H. Welch, Q.T. Phan, Y. Fu, A.S. Ibrahim, S.G. Filler, M. Zhang, A.J. Waring, J.E. Edwards, Jr., Functional and structural diversity in the Als protein family of *Candida albicans*, J. Biol. Chem. 279 (2004) 30480–30489.

[23] N. Sreerama, S.Y. Venyaminov, R.W. Woody, Estimation of the number of alpha-helical and beta-strand segments in proteins using circular dichroism spectroscopy, Protein Sci. 8 (1999) 370–380.

[24] A. Lobley, L. Whitmore, B.A. Wallace, DICHROWEB: an interactive website for the analysis of protein secondary structure from circular dichroism spectra, Bioinformatics 18 (2002) 211–212.

[25] W.K. Surewicz, H.H. Mantsch, New insight into protein secondary structure from resolution-enhanced infrared spectra, Biochim. Biophys. Acta 952 (1988) 115–130.

[26] E. Goormaghtigh, V. Raussens, J.M. Ruysschaert, Attenuated total reflection infrared spectroscopy of proteins and lipids in biological membranes, Biochim. Biophys. Acta 1422 (1999) 105–185.

[27] N. Guex, M.C. Peitsch, SWISS-MODEL and the Swiss-PdbViewer: an environment for comparative protein modeling, Electrophoresis 18 (1997) 2714–2723.

[28] T. Schwede, J. Kopp, N. Guex, M.C. Peitsch, SWISS-MODEL: an automated protein homology-modeling server, Nucleic Acids Res. 31 (2003) 3381–3385.

[29] X. Huang, W. Miller, A time-efficient, linear-space local similarity algorithm, Adv. Appl. Math. 12 (1991) 337–367.

[30] C.M. Topham, P. Thomas, J.P. Overington, M.S. Johnson, F. Eisenmenger, T.L. Blundell, An assessment of COMPOSER: a rule-based approach to modelling protein structure, Biochem. Soc. Symp. 57 (1990) 1–9.

[31] A. Godzik, A. Kolinski, J. Skolnick, Topology fingerprint approach to the inverse protein folding problem, J. Mol. Biol. 227 (1992) 227–238.

[32] L. Jaroszewski, L. Rychlewski, B. Zhang, A. Godzik, Fold prediction by a hierarchy of sequence, threading, and modeling methods, Protein Sci. 7 (1998) 1431–1440.

[33] W.D. Cornell, P. Cieplak, C.I. Bayly, I.R. Gould, K.M. Merz, D.M. Ferguson, D.C. Spellmeyer, T. Fox, J.W. Caldwell, P.A. Kollman, A

second generation force field for the simulation of proteins, nucleic acids, and organic molecules, J. Am. Chem. Soc. 117 (1995) 5179–5197.

[34] W. Heiden, T. Goetze, J. Brickmann, Fast generation of molecular surfaces from 3D data fields with an enhanced "marching cube" algorithm, J. Comput. Chem. 14 (1993) 246–250.

[35] G.E. Kellogg, S.F. Semus, D.J. Abraham, HINT: a new method of empirical hydrophobic field calculation for CoMFA, J. Comput. Aided Mol. Des. 5 (1991) 545–552.

[36] X. Zhang, L. Chen, D.P. Bancroft, C.K. Lai, T.E. Maione, Crystal structure of recombinant human platelet factor 4, Biochemistry 33 (1994) 8361–8366.

[37] V.K. Dhawan, A.S. Bayer, M.R. Yeaman, Thrombin-induced platelet microbicidal protein susceptibility phenotype influences the outcome of oxacillin prophylaxis and therapy of experimental *Staphylococcus aureus* endocarditis, Antimicrob. Agents Chemother. 44 (2000) 3206–3209.

[38] M.R. Yeaman, D. Cheng, B. Desai, L.I. Kupferwasser, Y.Q. Xiong, K.D. Gank, J.E. Edwards Jr., A.S. Bayer, Susceptibility to thrombin-induced platelet microbicidal protein is associated with increased fluconazole efficacy against experimental endocarditis due to *Candida albicans*, Antimicrob. Agents Chemother. 48 (2004) 3051–3056.

[39] A. Bjorstad, H. Fu, A. Karlsson, C. Dahlgren, J. Bylund, Interleukin-8-derived peptide has antibacterial activity, Antimicrob. Agents Chemother. 49 (2005) 3889–3895.

[40] R.P. Darveau, J. Blake, C.L. Seachord, W.L. Cosand, M.D. Cunningham, L. Cassiano-Clough, G. Maloney, Peptides related to the carboxyl terminus of human platelet factor IV with antibacterial activity, J. Clin. Invest. 90 (1992) 447–455.

[41] T. Lejon, J.S. Svendsen, B.E. Haug, Simple parameterization of non-proteinogenic amino acids for QSAR of antibacterial peptides, J. Pept. Sci. 8 (2002) 302–306.

[42] R.I. Lehrer, A.K. Lichtenstein, T. Ganz, Defensins: antimicrobial and cytotoxic peptides of mammalian cells, Annu. Rev. Immunol. 11 (1993) 105–128.

[43] A.V. Panyutich, P.S. Hiemstra, S. van Wetering, T. Ganz, Human neutrophil defensin and serpins form complexes and inactivate each other, Am. J. Respir. Cell Mol. Biol. 12 (1995) 351–357.

[44] V. Booth, D.W. Keizer, M.B. Kamphuis, I. Clark-Lewis, B.D. Sykes, The CXCR3 binding chemokine IP-10/CXCL10: structure and receptor interactions, Biochemistry 41 (2002) 10418–10425.

[45] V. Booth, C.M. Slupsky, I. Clark-Lewis, B.D. Sykes, Unmasking ligand binding motifs: identification of a chemokine receptor motif by NMR studies of antagonist peptides, J. Mol. Biol. 327 (2003) 329–334.

[46] N.Y. Yount, J. Yuan, A. Tarver, T. Castro, G. Diamond, P.A. Tran, J.N. Levy, C. McCullough, J.S. Cullor, C.L. Bevins, M.E. Selsted, Cloning and expression of bovine neutrophil beta-defensins. Biosynthetic profile during neutrophilic maturation and localization of mature peptide to novel cytoplasmic dense granules, J. Biol. Chem. 274 (1999) 26249–26258.

[47] N.Y. Yount, M.S. Wang, J. Yuan, N. Banaiee, A.J. Ouellette, M.E. Selsted, Rat neutrophil defensins. Precursor structures and expression during neutrophilic myelopoiesis, J. Immunol. 155 (1995) 4476–4484.

[48] M.H. Braff, M.A. Hawkins, A. Di Nardo, B. Lopez-Garcia, M.D. Howell, C. Wong, K. Lin, J.E. Streib, R. Dorschner, D.Y. Leung, R.L. Gallo, Structure–function relationships among human cathelicidin peptides: dissociation of antimicrobial properties from host immunostimulatory activities, J. Immunol. 174 (2005) 4271–4278.

[49] M.I. van der Kraan, K. Nazmi, A. Teeken, J. Groenink, W. van 't Hof, E.C. Veerman, J.G. Bolscher, A.V. Nieuw Amerongen, Lactoferrampin, an antimicrobial peptide of bovine lactoferrin, exerts its candidacidal activity by a cluster of positively charged residues at the C-terminus in combination with a helix-facilitating N-terminal part, Biol. Chem. 386 (2005) 137–142.

[50] M. Motizuki, T. Itoh, T. Satoh, S. Yokota, M. Yamada, S. Shimamura, T. Samejima, K. Tsurugi, Lipid-binding and antimicrobial properties of synthetic peptides of bovine apolipoprotein A-II, Biochem. J. 342 (Pt 1) (1999) 215–221.

[51] M. Dathe, T. Wieprecht, Structural features of helical antimicrobial peptides: their potential to modulate activity on model membranes and biological cells, Biochim. Biophys. Acta 1462 (1999) 71–87.

[52] K.J. Hallock, D.K. Lee, A. Ramamoorthy, MSI-78, an analogue of the magainin antimicrobial peptides, disrupts lipid bilayer structure via positive curvature strain, Biophys. J. 84 (2003) 3052–3060.

[53] K.A. Henzler-Wildman, G.V. Martinez, M.F. Brown, A. Ramamoorthy, Perturbation of the hydrophobic core of lipid bilayers by the human antimicrobial peptide LL-37, Biochemistry 43 (2004) 8459–8469.

[54] K.A. Henzler Wildman, D.K. Lee, A. Ramamoorthy, Mechanism of lipid bilayer disruption by the human antimicrobial peptide, LL-37, Biochemistry 42 (2003) 6545–6558.

[55] A. Mecke, D.K. Lee, A. Ramamoorthy, B.G. Orr, M.M. Banaszak Holl, Membrane thinning due to antimicrobial peptide binding: an atomic force microscopy study of MSI-78 in lipid bilayers, Biophys. J. 89 (2005) 4043–4050.

[56] F. Porcelli, B.A. Buck-Koehntop, S. Thennarasu, A. Ramamoorthy, G. Veglia, Structures of the dimeric and monomeric variants of magainin antimicrobial peptides (MSI-78 and MSI-594) in micelles and bilayers, determined by NMR spectroscopy, Biochemistry 45 (2006) 5793–5799.

[57] F. Porcelli, B. Buck, D.K. Lee, K.J. Hallock, A. Ramamoorthy, G. Veglia, Structure and orientation of pardaxin determined by NMR experiments in model membranes, J. Biol. Chem. 279 (2004) 45815–45823.

[58] Y.Q. Xiong, A.S. Bayer, L. Elazegui, M.R. Yeaman, A synthetic congener modeled on a microbicidal domain of thrombin-induced platelet microbicidal protein 1 recapitulates staphylocidal mechanisms of the native molecule, Antimicrob. Agents Chemother. 50 (2006) 3786–3792.

[59] A. Pellegrini, Antimicrobial peptides from food proteins, Curr. Pharm. Des. 9 (2003) 1225–1238.

[60] S.A. Kristian, M. Durr, J.A. Van Strijp, B. Neumeister, A. Peschel, MprF-mediated lysinylation of phospholipids in *Staphylococcus aureus* leads to protection against oxygen-independent neutrophil killing, Infect. Immun. 71 (2003) 546–549.

[61] R.A. Maxwell, W.H. Welch, F.M. Horodyski, K.M. Schegg, D.A. Schooley, Juvenile hormone diol kinase. II. Sequencing, cloning, and molecular modeling of juvenile hormone-selective diol kinase from *Manduca sexta*, J. Biol. Chem. 277 (2002) 21882–21890.

[62] M.R. Yeaman, N.Y. Yount, Mechanisms of antimicrobial peptide action and resistance, Pharmacol. Rev. 55 (2003) 27–55.